

# On the observability of coupled dark energy with cosmic voids

P. M. Sutter<sup>1,2,3</sup> \*, Edoardo Carlesi<sup>4</sup>, Benjamin D. Wandelt<sup>1,2,5,6</sup>, and Alexander Knebe<sup>4</sup>,

<sup>1</sup> Sorbonne Universités, UPMC Univ Paris 06, UMR7095, Institut d’Astrophysique de Paris, F-75014, Paris, France

<sup>2</sup> CNRS, UMR7095, Institut d’Astrophysique de Paris, F-75014, Paris, France

<sup>3</sup> Center for Cosmology and Astro-Particle Physics, Ohio State University, Columbus, OH 43210

<sup>4</sup> Departamento de Física Teórica, Universidad Autónoma de Madrid, 28049, Cantoblanco, Madrid, Spain

<sup>5</sup> Department of Physics, University of Illinois at Urbana-Champaign, Urbana, IL 61801

<sup>6</sup> Department of Astronomy, University of Illinois at Urbana-Champaign, Urbana, IL 61801

3 May 2022

## ABSTRACT

Taking  $N$ -body simulations with volumes and particle densities tuned to match the SDSS DR7 spectroscopic main sample, we assess the ability of current void catalogs (e.g., Sutter et al. 2012b) to distinguish a model of coupled dark matter-dark energy from  $\Lambda$ CDM cosmology using properties of cosmic voids. Identifying voids with the VIDE toolkit, we find no statistically significant differences in the ellipticities, but find that coupling produces a population of significantly larger voids, possibly explaining the recent result of Tavasoli et al. (2013). In addition, we use the universal density profile of Hamaus et al. (2014) to quantify the relationship between coupling and density profile shape, finding that the coupling leads to deeper underdensities for medium-scale voids and broader, shallower, undercompensated profiles for large voids. We find that these differences are potentially measurable with existing void catalogs once effects from survey geometries and peculiar velocities are taken into account.

**Key words:** cosmology: simulations, cosmology: large-scale structure of universe

## 1 INTRODUCTION

Even though a variety of cosmological tests demonstrate that the inflation plus cold dark matter ( $\Lambda$ CDM) paradigm is extremely successful in describing the history and structure of the Universe (e.g., Reid et al. 2012; Planck Collaboration 2013), there are still several features of the large-scale distribution of matter that are difficult to explain. One is the so-called “void phenomenon”, first noticed by Peebles (2001), in which cosmic voids — the deep underdensities in the galaxy distribution — appear emptier than expected from  $N$ -body simulations.

The observation of this phenomenon motivated the development of models in which a dynamical scalar field responsible for dark energy (DE; Peebles & Ratra 1988; Ratra & Peebles 1988) is coupled to the dark matter (DM), giving an additional fifth force of nature that would help empty out the voids (Nusser et al. 2005). Other possibilities to explain the void phenomenon have since been proposed, including modified gravity (e.g., Li & Zhao 2009; Clampitt

et al. 2013; Spolyar et al. 2013) and an improved understanding of the relationship between galaxy formation and environment (Tinker & Conroy 2009; Kreckel et al. 2011).

Most analyses of coupled DM-DE have focused on the statistics of overdense regions, such as the halo mass function (Sutter & Ricker 2008; Cui et al. 2012), the galaxy two-point correlation function (Carlesi et al. 2013) and galaxy cluster gas properties (Baldi et al. 2010; Carlesi et al. 2013). However, in these high-density environments it is difficult to distinguish effects due to coupling from non-linear evolution and complex baryonic physics.

Focusing on underdense regions would appear to be a more natural way to study the void phenomenon. On the theory side, studies have considered the effect of coupling in the dark sector on the void number function (Clampitt et al. 2013) and density profile (Spolyar et al. 2013), and simulations of the effects of fifth forces on void shapes (Li & Zhao 2009; Li et al. 2012). Observationally, void populations in galaxy surveys can be compared to expectations from simulations (e.g., Muller et al. 2000; Pan et al. 2012). Most recently, the study of Sutter et al. (2013) found no evidence for departures from  $\Lambda$ CDM for a population of voids

\* Email: sutter@iap.fr

at higher redshift ( $z \sim 0.4 - 0.7$ ), but Tavasoli et al. (2013) noted the existence of a large void that appears to be statistically incompatible with predictions of  $\Lambda$ CDM  $N$ -body simulations.

This relative inattention to voids themselves can be explained by the relative dearth of voids in observations and the lack of robust void statistical tools that can be used to connect theoretical results to observational reality. However, there have been significant advancements in the past few years, including the release of large public void catalogs (Pan et al. 2012; Sutter et al. 2012, 2013) from the SDSS galaxy surveys (Abazajian et al. 2009; Ahn et al. 2012). Secondly, there has been significant efforts to single out especially sensitive void properties and make predictions for the void signals in data (e.g., Lavaux & Wandelt 2010; Biswas et al. 2010; Bos et al. 2012; Jennings et al. 2013; Sutter et al. 2013). The combination of enhanced tools and a statistically meaningful sample of voids means that predictions of the effects of coupled DM-DE within voids can now make direct contact with data.

In this *letter* we provide an initial assessment of the impact of coupled DM-DE on void statistics such as number functions, ellipticities, and radial density profiles. While this work is similar to that of Li (2011), we particularly focus on the ability of current low-redshift galaxy surveys such as the SDSS DR7 (Ahn et al. 2012) to distinguish coupled models from  $\Lambda$ CDM with the population of voids identified in their limited volumes and galaxy densities (Pan et al. 2012; Sutter et al. 2012). We also incorporate the latest theoretical work, such as the recently-described universal density profile (Hamaus et al. 2014; hereafter HSW), to understand and quantify our results.

In the following section we briefly present the quintessence model, its implementation in simulation, and our method for finding voids. In Section 3 we discuss the effects on void properties, and conclude in Section 4 with comments on the relevancy for current surveys and outline strategies for more complete analyses in the future.

## 2 SIMULATIONS & VOID FINDING

Under quintessence the dark energy scalar field  $\phi$  has the Lagrangian

$$L = \int d^4x \sqrt{-g} v \left( -\frac{1}{2} \partial_\mu \phi \partial^\mu \phi + V(\phi) + m(\phi) \psi_m \bar{\psi}_m \right), \quad (1)$$

where  $\phi$  interacts with the matter field  $\psi_m$  through the mass term of the dark matter particles. In this work we assume the Ratra & Peebles (1988) self interaction potential:

$$V(\phi) = V_0 \left( \frac{\phi}{M_p} \right)^{-\alpha} \quad (2)$$

where  $M_p$  is the Planck mass and  $V_0$  and  $\alpha$  are two parameters that must be fixed by fitting to observations (Wang et al. 2012; Chiba et al. 2013).

Under this interaction the dark matter particle mass evolves as

$$m(\phi) = m_0 \exp \left( -\beta(\phi) \frac{\phi}{M_p} \right). \quad (3)$$

This evolution implies that the dark matter particles experience an effective gravitational constant of the form (Baldi

et al. 2010):

$$\tilde{G} = G_N (1 + 2\beta^2(\phi)) \quad (4)$$

where  $G_N$  is the standard Newtonian value. We will fix the interaction term to be constant such that  $\beta(\phi) = \beta_0$ . This leads to a dark matter particle mass that decreases as a function of time to its  $z = 0$   $\Lambda$ CDM value. For this work, we contrast a  $\Lambda$ CDM case with a single interacting model with parameters  $V_0 = 10^{-7}$ ,  $\alpha = 0.143$ , and  $\beta = 0.099$  (hereafter referred to as cDE).

We used the simulations described in Carlesi et al. (2013) and Carlesi et al. (2013) for this analysis. Briefly, these interactions were implemented with a modified version of the Tree-PM code **GADGET-2** (Springel 2005), with initial conditions generated using a version of the **N-GenIC** code suitably modified to account for the interactions. The cosmological parameters used in both  $\Lambda$ CDM and cDE simulations were  $h = 0.7$ ,  $n = 0.951$ ,  $\Omega_{dm} = 0.224$ ,  $\Omega_b = 0.046$ , and  $\sigma_8 = 0.8$  (normalized at  $z = 0$ ) and were constructed to have dark matter power spectra within current observational limits.

These simulations took place in a cubic volume of  $250 h^{-1} \text{Mpc}$  per side using  $1024^3$  DM and  $1024^3$  gas particles. For this analysis we ignore the gas particles and randomly subsampled the  $z = 0.1$  dark matter particles to achieve a mean density of  $\bar{n} = 4 \times 10^{-3}$  per cubic  $h^{-1} \text{Mpc}$ . This combination of simulation volume, density, and redshift approximates the *dim2* volume-limited SDSS galaxy sample used in the void catalog of Sutter et al. (2012). We subsample the simulations to have identical numbers of particles; this way, both the first order (number density) and second order (correlation function) statistics are identical; we are performing a ‘‘controlled experiment’’ to examine the effects of coupling on voids. Even though this study ignores the effects of galaxy bias, Sutter et al. (2013) found that bias does not greatly impact void density profiles and abundances. In other words, to examine the impact of DM-DE coupling in a realistic scenario we may ignore galaxy (and halo) bias and work only subsampled dark matter populations.

We identify voids with a heavily modified version of ZOBOV (Neyrinck 2008). The modifications are described extensively in Sutter et al. (2014), and we call this enhanced code **VIDE**, for Void IDentification and Examination. This approach begins with a Voronoi tessellation of the tracer particles to construct a density field and uses the watershed transform to group Voronoi cells into zones and voids (Platen et al. 2007). As in Sutter et al. (2012), we remove voids smaller than the mean particle separation ( $6.3 h^{-1} \text{Mpc}$ ) and those with central densities higher than 0.2 the mean particle density  $\bar{n}$ . Additionally, to limit the growth of voids we set a threshold of  $0.2\bar{n}$  for joining additional zones into voids (see Neyrinck (2008) for a discussion). If a void consists of only a single zone (as they often do in sparse populations) then this restriction does not apply.

We will take as the center of each void the volume-weighted center, or *macrocenter*:

$$\mathbf{x}_v = \frac{1}{\sum_i V_i} \sum_i \mathbf{x}_i V_i, \quad (5)$$

where  $\mathbf{x}_i$  and  $V_i$  are the positions and Voronoi volumes of each tracer  $i$ , respectively.

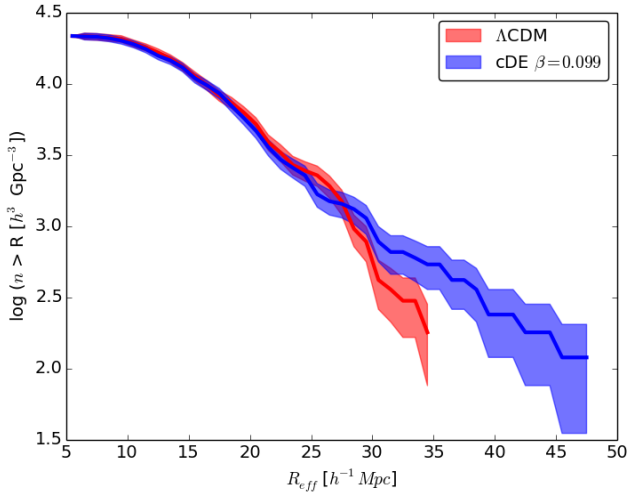


**Figure 1.** Cumulative void number functions. Shown are abundances for  $\Lambda$ CDM (red) and cDE (blue) models from subsampled  $N$ -body simulations. The solid lines are the measured number functions and the shaded regions are the  $1\sigma$  Poisson uncertainties. For the same  $\sigma_8$ , cDE results in an excess of large scale voids and a deficit of medium scale voids compared to  $\Lambda$ CDM.

### 3 RESULTS

While DM-DE coupling will have myriad effects on void properties (Li & Zhao 2009; Li et al. 2012), we will focus on three key statistics: abundances, ellipticities, and radial density profiles. These represent especially sensitive probes of alternative cosmologies (e.g., Bos et al. 2012) and are well understood in both data and simulations (e.g., Sutter et al. 2013).

Figure 1 shows the cumulative number function for the  $\Lambda$ CDM and cDE simulations. We immediately note the presence of large voids in the cDE simulation, well beyond the largest voids in the  $\Lambda$ CDM simulation. However, for smaller void sizes ( $R_{\text{eff}} < 20 h^{-1}\text{Mpc}$ ) the two void populations are almost indistinguishable. This makes sense if the DM-DE coupling affects voids by inflating them beyond their typical  $\Lambda$ CDM sizes: since small voids just become medium-scale voids under the influence of cDE, and there is a large reservoir of very small voids, the number functions will be identical until the larger scales, where the greatest  $\Lambda$ CDM voids become even larger with cDE. The total number of voids in both models is nearly the same due to our fixing of  $\sigma_8 = 0.8$  in both models.

In Figure 2 we show one-dimensional radial profiles for all samples in a few selected radius ranges. To compute the profiles, we take all voids in a sample of a given size range (e.g.,  $30 - 35 h^{-1}\text{Mpc}$ ), align all their macrocenters (Eq. 5), and measure the density in thin spherical shells. We normalize each density profile to the mean number density of the sample and show all profiles as a function of relative radius,  $R/R_v$ , where  $R_v$  is the median void size in the stack. We only stack voids above  $2R_{\text{eff,min}}$  and if there were at least 10 voids in the stack; otherwise there is an insufficient number of particle to build a density profile. These operations are identical to the procedure performed in data (Sutter et al. 2012, 2013), where we do not know *a priori* what cosmology we are observing. Thus this is the approach we take

when comparing theory to observations. Note that there is an additional stack of the largest voids in the cDE model not available in the  $\Lambda$ CDM case.

The profiles in each stack follow the same overall structure (a deeply-underdense core, a steep wall, an overdense “compensation” shell, and a flattening to the mean density); however, there are some differences between  $\Lambda$ CDM and cDE voids. First, cDE voids appear slightly more underdense for the smallest stacks, although the overall sizes are not significantly different. The greatest discrepancies appear for the larger ( $> 20 h^{-1}\text{Mpc}$ ) stacks. From 20 to  $25 h^{-1}\text{Mpc}$ , cDE voids have slightly higher compensation shells, but after  $25 h^{-1}\text{Mpc}$  the cDE voids are clearly larger and flatter (i.e., lower density contrast between wall and center).

To quantify and understand these differences, we fit all the profiles to the universal function presented in HSW:

$$\frac{n}{\bar{n}}(r) = \delta_c \frac{1 - (r/r_s)^{\alpha(r_s)}}{1 + (r/R_v)^{\beta(r_s)}} + 1, \quad (6)$$

While there are four parameters total in the model, HSW describe a two-parameter reduced model where

$$\alpha(r_s) \simeq -2.0(r_s/R_v) + 4.0 \quad (7)$$

$$\beta(r_s) \simeq \begin{cases} 17.5(r_s/R_v) - 6.5 & \text{if } r_s/R_v < 0.91 \\ -9.8(r_s/R_v) + 18.4 & \text{if } r_s/R_v > 0.91. \end{cases} \quad (8)$$

This two-parameter model describes all but the largest voids very accurately, and is appropriate for the analysis here (Sutter et al. 2013). There are two free parameters to this model:  $r_s$ , the radius at which the profile reaches mean density, and  $\delta_c$ , the density in the central core. Figure 3 shows all best-fit values of  $\delta_c$  and  $r_s$  for all stacks in both simulations. We also show in the figure the line between overcompensation and undercompensation as derived in HSW. In the figure, fits to smaller voids are on the left and fits to larger voids are on the right.

The fitting parameters elucidate the relationship between DM-DE coupling and profile shape.  $\Lambda$ CDM voids generally maintain a fixed core underdensity as they get larger, but mid-scale cDE voids appear more underdense (as they are presumably emptied out). This causes the higher compensation shells in the  $20 - 25 h^{-1}\text{Mpc}$  stack: the material from these voids has been deposited into the walls surrounding them. The largest voids under cDE get inflated well beyond their  $\Lambda$ CDM counterparts. Indeed, the largest cDE voids in this volume become undercompensated, whereas no  $\Lambda$ CDM voids reach the necessary scales to be undercompensated. For these voids, the entire void structure has been enlarged. This also fits with the dip in the number function at these same scales: small voids are largely unaffected, but medium-scale voids expand to become larger voids.

We also examined ellipticities using the inertia tensor method as described in Bos et al. (2012) and Sutter et al. (2013). However, as Bos et al. (2012) discovered, in sparse populations such as galaxies it is very difficult to statistically separate  $\Lambda$ CDM from alternative cosmologies using void shapes. We found no meaningful distinctions in the ellipticities, either globally or as a function of effective radius, of our two void populations.

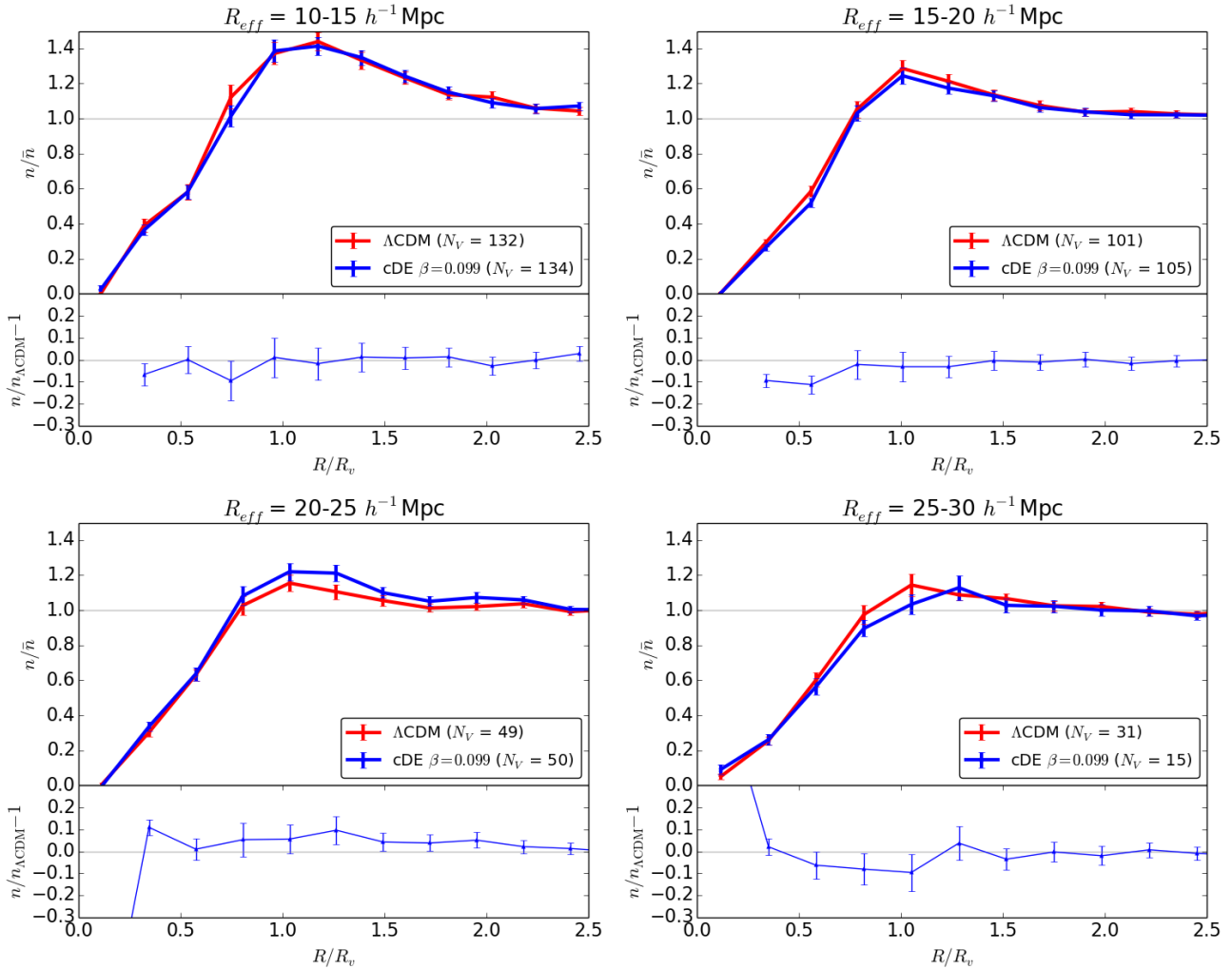


**Figure 2.** One-dimensional radial density profiles of stacked voids with  $1\sigma$  uncertainties (points with error bars). The bottom of each panel shows the cDE profile relative to the  $\Lambda$ CDM one. The solid lines are to guide the eye. Shown are profiles from the  $\Lambda$ CDM (red) and cDE (blue) simulations. The legend indicates the number of voids  $N_V$  used to construct the corresponding stack. Each profile is normalized to the mean number density  $\bar{n}$  of that sample and  $R_v$  corresponds to the median void size in the stack. We produce error bars by bootstrapping the voids in each stack. The thin grey line indicates mean  $\Lambda$ CDM. Coupling empties out medium scale voids, reducing their central densities and enhancing their compensation walls relative to  $\Lambda$ CDM.

#### 4 CONCLUSIONS

We have examined the effects on voids due to coupling between dark matter and dark energy with realistic galaxy survey volumes and tracer densities and provided an initial assessment of the feasibility of current surveys to detect the coupling with voids. We have found that the coupling produces much larger and underdense voids compared to  $\Lambda$ CDM mostly by inflating medium-scale voids while leaving the smallest voids (and the total number of voids) unaffected. Additionally, we have quantified the effects of coupling on the radial density profiles by finding the best fits to the analytic HSW profile, and found that DM-DE coupling can more easily make voids underdense.

Traditional probes of large-scale structure such as the power spectrum have difficulty differentiating cDE models from  $\Lambda$ CDM (e.g., Carlesi et al. 2013), but voids are exceptionally powerful discriminating tools. Even with limited survey volumes and only  $\sim 400$  total voids the number func-

tions and radial density profiles are distinguishable in a statistically significant manner.

The void population we have studied is fairly representative of — and accessible with — current low-redshift galaxy surveys (Sutter et al. 2012). These results may explain the large void identified in the analysis of Tavasoli et al. (2013). In addition, using Halo Occupation Distribution modeling (Berlind & Weinberg 2002) and accounting for survey geometries, Sutter et al. (2013) was able to match  $\Lambda$ CDM simulations to observed void populations. Thus, coupled DM-DE may already be measurable with current data sets. However, for a complete comparison of the void abundance we must include mask effects (Sutter et al. 2013). We also have not included the effects of galaxy bias and distortions to the density profiles from peculiar velocities. However, we can use techniques such as those presented by Pisani et al. (2013) to construct the real-space profile

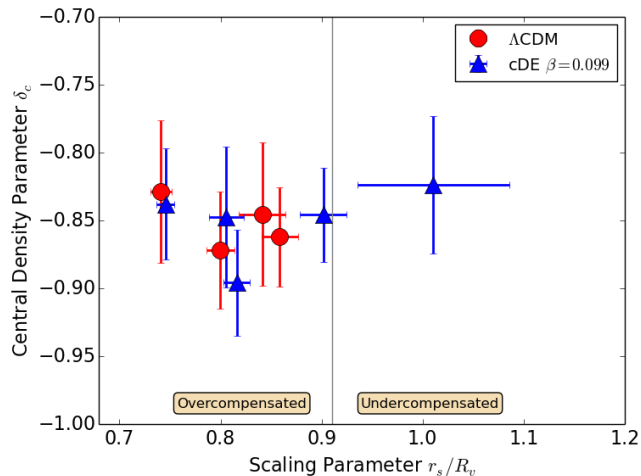


**Figure 3.** Best-fit values and  $1\sigma$  uncertainties for all void stacks studied using the profile given by Eq. (6). Shown are values from  $\Lambda$ CDM (red circles) and cDE (blue triangles). The thin grey line depicts the analytically-derived compensation scale. For each sample from left to right the points are for the  $10 - 15$ ,  $15 - 20$ ,  $20 - 25$ ,  $25 - 30$ , and  $35 - 40 h^{-1}\text{Mpc}$  stacks. Note that there is an additional stack of the largest voids in the cDE model not available in the  $\Lambda$ CDM case, while the very smallest voids remain relatively unaffected.

without modeling. We will save a more detailed comparison and measurement of a constraint for future work.

This study is only an initial assessment comparing one cDE model to  $\Lambda$ CDM, using simulations optimized to study the properties of high-density clusters. We also examined other coupling strengths (Eq. 4) but did not find significant differences among the models with this limited void population. We are preparing larger simulations that will allow us to examine the detailed relationship between coupling strength and void properties and assess the ability of high-redshift galaxy surveys such as BOSS (Dawson et al. 2013) to probe these cosmologies using voids.

## ACKNOWLEDGMENTS

PMS and EC thank Alexander Kusenko and the NSF for the PACIFIC2013 workshop, where this work was initiated. PMS and BDW acknowledge support from NSF Grant NSF AST 09-08693 ARRA. BDW acknowledges funding from an ANR Chaire d’Excellence (ANR-10-CEXC-004-01), the UPMC Chaire Internationale in Theoretical Cosmology, and NSF grants AST-0908 902 and AST-0708849. This work made in the ILP LABEX (under reference ANR-10-LABX-63) was supported by French state funds managed by the ANR within the Investissements d’Avenir programme under reference ANR-11-IDEX-0004-02.

AK is supported by the *Ministerio de Economía y Competitividad* (MINECO) in Spain through grant AYA2012-31101 as well as the Consolider-Ingenio 2010 Programme of the *Spanish Ministerio de Ciencia e Innovación* (MICINN) under grant MultiDark CSD2009-00064. He also acknowledges support from the *Australian Research Council* (ARC) grants DP130100117 and DP140100198. He further thanks Ghosts I’ve Met for winter’s ruin.

The authors thank Nico Hamaus, Alice Pisani, and Ravi Sheth for useful comments.

## REFERENCES

- Abazajian K. N., et al., 2009, *Astrophys. J. Supp.*, 182, 543  
 Ahn C. P., et al., 2012, *Astrophys. J. Supp.*, 203, 21  
 Baldi M., Pettorino V., Robbers G., Springel V., 2010, *Mon. Not. R. Astron. Soc.*, 403, 1684  
 Berlind A. A., Weinberg D. H., 2002, *ApJ*, 575, 587  
 Biswas R., Alizadeh E., Wandelt B., 2010, *Phys. Rev. D*, 82  
 Bos E. G. P., van de Weygaert R., Dolag K., Pettorino V., 2012, *ArXiv e-prints*: 1205.4238  
 Carlesi E., Knebe A., Lewis G., Yepes G., 2013  
 Carlesi E., Knebe A., Lewis G., Yepes G., Wales S., 2013  
 Chiba T., De Felice A., Tsujikawa S., 2013, *Phys. Rev. D*, 87, 083505  
 Clampitt J., Cai Y.-C., Li B., 2013, *Mon. Not. R. Astron. Soc.*, 431, 749  
 Cui W., Baldi M., Borgani S., 2012, *Mon. Not. R. Astron. Soc.*, 424, 993  
 Dawson K. S., et al., 2013, *AJ*, 145, 10  
 Hamaus N., Sutter P. M., Wandelt B. D., 2014, *ArXiv e-prints*: 1403.5499  
 Jennings E., Li Y., Hu W., 2013, *Mon. Not. R. Astron. Soc.*, 434, 2167  
 Kreckel K., Ryan Joung M., Cen R., 2011, *ApJ*, 735, 132  
 Lavaux G., Wandelt B. D., 2010, *Mon. Not. R. Astron. Soc.*, 403, 1392  
 Li B., 2011, *Mon. Not. R. Astron. Soc.*, 441, 2615  
 Li B., Zhao G.-B., Koyama K., 2012, *Mon. Not. R. Astron. Soc.*, 421, 3481  
 Li B., Zhao H., 2009, *Phys. Rev. D*, 80  
 Muller V., Arbabi-Bidgoli S., Einasto J., Tucker D., 2000, *Mon. Not. R. Astron. Soc.*, 318, 280  
 Neyrinck M. C., 2008, *Mon. Not. R. Astron. Soc.*, 386, 2101  
 Nusser A., Gubser S. S., Peebles P., 2005, *Phys. Rev.*, D71, 083505  
 Pan D. C., Vogeley M. S., Hoyle F., Choi Y.-Y., Park C., 2012, *Mon. Not. R. Astron. Soc.*, 421, 926  
 Peebles P. J. E., 2001, *ApJ*, 557, 495  
 Peebles P. J. E., Ratra B., 1988, *ApJ*, 325, L17  
 Pisani A., Lavaux G., Sutter P. M., Wandelt B. D., 2013, *ArXiv e-prints*: 1306.3052  
 Planck Collaboration 2013, *ArXiv e-prints*: 1303.5076  
 Platen E., van de Weygaert R., Jones B. J. T., 2007, *Mon. Not. R. Astron. Soc.*, 380, 551  
 Ratra B., Peebles P. J. E., 1988, *Phys. Rev. D*, 37, 3406  
 Reid B. A., et al., 2012, *Mon. Not. R. Astron. Soc.*, 426, 2719  
 Spolyar D., Sahlén M., Silk J., 2013, *ArXiv e-prints*: 1304.5239  
 Springel V., 2005, *Mon. Not. R. Astron. Soc.*, 364, 1105  
 Sutter P. M., et al., 2014, (in prep)  
 Sutter P. M., Lavaux G., Wandelt B. D., Weinberg D. H., 2012, *ApJ*, 761, 44  
 Sutter P. M., Lavaux G., Wandelt B. D., Weinberg D. H., Warren M. S., 2013, *ArXiv e-prints*: 1310.7155  
 Sutter P. M., Lavaux G., Wandelt B. D., Hamaus N., Weinberg D. H., Warren M. S., 2013, *ArXiv e-prints*: 1309.5087  
 Sutter P. M., Ricker P. M., 2008, *ApJ*, 687, 7  
 Tavasoli S., Vasei K., Mohayaee R., 2013, *Astron. & Astrophys.*, 553, A15  
 Tinker J. L., Conroy C., 2009, *ApJ*, 691, 633  
 Wang P.-Y., Chen C.-W., Chen P., 2012, *Journal of Cosmology and Astroparticle Physics*, 2, 16